AAEC/TM335

COPY NO.

AUSTRALIAN ATOMIC ENERGY COMMISSION

RESEARCH ESTABLISHMENT

LUCAS HEIGHTS

OBSERVATIONS ON THE SINTERABILITY, STRENGTH, AND STRUCTURE OF VARIOUS GRADES OF BERYLLIUM OXIDE

by

T.E. CLARE

AUGUST 1966

AUSTRALIAN ATOMIC ENERGY COMMISSION

RESEARCH ESTABLISHMENT

LUCAS HEIGHTS

OBSERVATIONS ON THE SINTERABILITY, STRENGTH, AND STRUCTURE OF VARIOUS GRADES OF BERYLLIUM OXIDE

by

T.E. CLARE

ABSTRACT

Four sulphate-derived beryllia powders from three different commercial sources have been isostatically pressed and sintered. These powders showed significant variations in sintering behaviour which could be partially predicted by semi-empirical equations taking physical properties of the powder into account; the limitations of these equations are discussed.

High strength is associated with high density, fine grained, and flaw-free sintered materials, and the four powders examined could be placed in a high or low strength category from a cursory glance at their microstructure. However, an overall correlation between purity and physical properties of powders, sinterability of compacts, and strength and microstructure of sintered compacts cannot be anticipated at the present stage of knowledge of sintering of ceramics.

CONTENTS

		Page
1.	INTRODUCTION	1
2.	EXPERIMENTAL	1
	2.1 Materials	1
	2.2 Preparation of Specimens	1
	2.3 Sintering	2
	2.4 Density Determination	2
	2.5 Machining	2
	2.6 Modulus of Rupture Determination	2
	2.7 Metallography and Grain Size Measurement	3
3.	RESULTS	3
	3.1 Sinterability	3
	3.2 Strength	3
	3.3 Structure	4
4.	DISCUSSION	4
	4.1 Sinterability	4
	4.1.1 Purity	5
	4.1.2 Surface area and green density	5
	4.1.3 Effect of compaction pressure	6
	4.1.4 Effect of Milling	6
	4.2 Structure	7
	4.2.1 Defects	7
	4.2.2 Grain size versus porosity	7
	4.3 Strength	8
	4.3.1 Strength-porosity relationship	8
	4.3.2 Strength-grain size relationship	9
	4.3.3 Strength-compaction pressure relationship	10
	4.3.4 Effect of 'macro'-defects on strength	10
	4.3.5 General remarks on the strength of powders A and B	10
5.	SUMMARY	11
6.	CONCLUSION	12
7.	ACKNOWLEDGEMENTS	13
8.	REFERENCES	
Appendix 1 -	Determination of Pour Density and Tap Density of BeO Powders	

Table 1 - Sources and analyses of beryllia powders

Table 2 - Physical properties

Figure 1 - Density after sintering at temperature for one hour

Figure 2 - Effect of compacting pressure on green and sintered densities of powders A and B

Figure 3 - A comparison of the sinterability of powders A and B

Figure 4 - Modulus of rupture versus porosity

Figure 5 - Modulus of rupture versus grain size

Figure 6 - Effect of compacting pressure on modulus of rupture of powders A and B

Figure 7 - Grain size versus porosity

Figure 8 - Powder A sintered for 3h at 1450°C, density 2.85 g/cm^3

Figure 9 - Powder B sintered for 6h at 1350°C, density 2.87 g/cm^3

Figure 10 - Powder C sintered for 3h at 1450°C, density 2.87 g/cm^3

Figure 11 - Powder D sintered for 2h at 1315°C, density 2.87 g/cm^3

Figure 12 - Powder C density 2.93 g/cm^3
grain size 9 microns
modulus of rupture 17,875 lb/in^2

Figure 13 - Powder B density 2.95 g/cm^3
grain size 7 microns
modulus of rupture 30,090 lt/in^2

Figure 14 - Powder D pressed at 20 tons/in^2, sintered to a density of 2.87 g/cm^3

Figure 15 - Electron photomicrographs of powders A and B pressed at 20 tons/in^2 and sintered

1. INTRODUCTION

This work was undertaken to provide further technological and scientific background to an established isostatic pressing and sintering process for BeO (Reeve and Ramm 1961; Reeve and Bridgford 1964). Nuclear grade beryllia powders show significant variations in properties and behaviour even between different batches of nominally the same grade of powder. With present knowledge, it is often impossible to predict variations in sintering behaviour in advance, and a continuing assessment of commercial nuclear-pure BeO powders is therefore necessary in any fabrication programme such as that which forms part of the A.A.E.C.'s High Temperature Gas-Cooled Reactor feasibility study.

In the present work, four BeO powders (two of nominally the same grade) were studied with the specific aims of (i) observing differences in powder properties, fabrication behaviour, and sintered properties and (ii) explaining the reasons for these differences. Some comments on the technological importance of the results are also made.

2. EXPERIMENTAL

2.1 Materials

The most readily available powders of sinterable quality and reactor grade purity are all sulphate-derived. The sources and analyses of the beryllia powders examined are shown in Table 1. Table 2 gives surface areas determined by the BET (nitrogen adsorption) technique, pour and tap densities determined as described in Appendix 1, some observations on the shape and size of the powders as seen by transmission optical microscopy, and the green density of compacts after isostatic pressing at 20 tons/in^2.

Most of the work described was on powders A and B, which are two representative batches of a widely accepted commercial BeO powder. Work on powders C and D was somewhat less extensive.

2.2 Preparation of Specimens

Powder A was milled in a polythene container with beryllia cylinders (density 2.90 g/cm^3, grain size 3 microns). The milled powder was thoroughly

dried to less than 1 per cent. moisture, and isostatically pressed without binder at 7, 10 and 20 tons/in^2. Powder B was isopressed at 2,4,7, 10 and 20 tons/in^2 without any prior milling. Powder C was pressed at 20 tons/in^2 only, without prior milling. Powder D was pressed with and without prior milling at 20 tons/in^2 only. All compacts were dried for 24 hours at 110°C, and stored in a desiccator to await sintering.

2.3 Sintering

A platinum/40 per cent. rhodium wound tube furnace (2 in. diameter) was used to sinter compacts at temperatures of 1550°C or below; at temperatures above 1550°C, an induction-heated graphite susceptor tube furnace was used. Each furnace contained a recrystallised alumina work tube ($1\frac{1}{2}$ in. diameter). Ten specimens could be sintered at one time in a 3 in. long uniform hot zone ($\pm$ 5°C), with an 80 per cent. platinum/20 per cent. rhodium versus 95 per cent. platinum/5 per cent. rhodium thermocouple placed in a central position. The furnace work tube was evacuated to less than 10^{-3} mmHg pressure, and heated to 800°C. At this temperature, the tube was filled with dry (< 100 p.p.m. H_2O) nitrogen to one atmosphere pressure and isolated. The furnace temperature was then increased to the desired sintering temperature at 400°C per hour, and held for the desired time. Specimens were furnace-cooled in nitrogen.

2.4 Density Determination

Green densities of compacts were determined by weighing and measuring and are reported as the arithmetic mean of two measurements on different compacts. The bulk densities and open porosities of all compacts in a sintered batch (10 specimens) were determined by water displacement. The values quoted are the arithmetic mean of a batch.

2.5 Machining

Each sintered specimen was centreless ground to 0.160 in. diameter using silicon carbide wheels (grit size 90 B.S.S.) and finally annealed at 800°C for 4 hours in air, to remove all machining coolant.

2.6 Modulus of Rupture Determination

Machined and annealed cylinders (1 in. x 0.160 in. dia.) were fractured at room temperature in four-point loading, over a 3/16 in. span and

5/16 in. gauge length, at a cross head speed of 0.05 in/min. on a Tinius Olsen Universal Testing Machine.

2.7 Metallography and Grain Size Measurement

Representative fracture surfaces (from modulus of rupture determinations) were polished with gamma-alumina on a Syntron vibratory polishing machine for approximately four days. The polished faces were etched in 10 per cent. ammonium bifluoride for $\frac{1}{2}$ hour and examined by optical and electron microscopy. Grain sizes smaller than 3 microns were determined by counting the number of grain boundary intercepts across electron photomicrographs, using magnifications which gave 12-24 grains along a chosen line; 100-200 grains were counted on each photomicrograph. Grain sizes above 3 microns were determined by similar grain boundary intercept counts under the optical microscope.

3. RESULTS

3.1 Sinterability

Bulk densities of the four grades of BeO after compacting at 20 tons/in^2 and sintering for 1 hour at temperatures from 1300°C to 1700°C are shown in Figure 1. At any sintering temperature, the sintered density of the four powders follows the order D>B>A>C.

The relationship between green and sintered densities and compacting pressure for powders A and B is shown in Figure 2. No limiting green or sintered density is observed at compacting pressures up to 20 tons/in^2 and the green and sintered densities of B are higher than those of A at all pressures.

The effect of sintering time on the sintered density of powders A and B at several sintering temperatures is shown in Figure 3. Powder A reaches a limiting sintered density in approximately 3 to 4 hours, whereas powder B continues to densify even after 6 hours.

3.2 Strength

Strength versus porosity for all powders is plotted in Figure 4 and strength versus grain size for powders A and B is plotted in Figure 5.

At equivalent porosities, the strength generally decreases in the order A>B>D>C. At equivalent grain size A is stronger than B. The strength

D is improved by milling the original powder and the order of strength then A>D (milled)>B>C (Figure 4).

The modulus of rupture versus density for several compaction essures is plotted for powders A and B in Figure 6. Accepting an apparently evitable scatter in modulus of rupture determinations (Veevers and Rotsey 65) there may be an increase in strength with increase in compaction pressure. modulus of rupture of both powders A and B is at a maximum in the density ge 2.85 - 2.90 g/cm^3.

3.3 Structure

Sintered grain sizes of specimens from all powders are shown in the in size versus porosity plots of Figure 7.

Photomicrographs of the four materials after pressing at 20 tons/in^2 sintering to approximately 95 per cent. of theoretical density are compared Figures 8 - 11. Perfectly uniform microstructures are not produced from of the powders; A and B contain many large acicular grains scattered in ine-grained matrix, C contains scattered areas of large grain size in a e-grained matrix, while D retains evidence of incomplete bonding between ginal powder agglomerates and has a non-uniform grain size. Powder C also ains large pores at triple points (Figure 12), and grain 'pull-out' during shing indicates a grain boundary weakness in the structure. Grain 'pull- is not observed in powders A and B (Figure 13), or in D.

In 'as-received' powder D, the bonding between agglomerates improves he sintered density increases. At 2.87 g/cm^3 the boundaries between omerates are very pronounced, at 2.91 g/cm^3 they are only just visible, at 2.95 g/cm^3 they have almost disappeared.

By milling powder D before compacting, a much more uniform structure btained on sintering (Figure 14b), the 'mottled' effect (Figure 14a) ppears, and there is no longer a low density, small grain size network.

DISCUSSION

4.1 Sinterability

An explanation of the observed order of sinterability (D>B>A>C for ons/in^2) can be sought in the physical and chemical properties of the powders.

4.1.1 Purity

All four powders were of "nuclear" purity, containing less than 500 p.p.m. of foreign cations. No individual cation was present at a level greater than 100 p.p.m. While larger variations in cationic impurity are known to be significant in affecting sinterability (Beaver et al. 1964; Livey and Hey 1964), there are no experimental results in this very low range of cationic impurity content, nor is there any evidence that moderately large contents of carbon or sulphur have outstanding effects on sinterability. In the present assessment, it is therefore assumed that the four powders do not differ significantly in impurity content.

4.1.2 Surface area and green density

If surface area is taken as a criterion, with high surface area powders showing better sinterability, the order predicted should be D>(B and A)>C, with B slightly better than A. In fact, A and C are observed to be much closer in sinterability than A and B (Figure 1). Inspection of Table 2 and Figure 1 shows that no other physical property can alone explain the observed behaviour.

A relationship taking both surface area and green density into account in predicting sinterability for sulphate-derived nuclear-pure powders has recently been proposed by Bannister (1965). This relationship is:

$$10^4/T = 3.4 + 2.8 \log_{10} S - 6 \log_{10}(3.01 - D_o), \quad \ldots\ldots (1)$$

where T = temperature in ^oK to reach a density of 2.90 g/cm^3 after sintering for 1 hour at that temperature in dry N_2,

S = surface area, m^2/g ,

D_o = green density, g/cm^3 .

If this relationship is now used to predict "sintering temperatures" of powders A,B,C,D pressed at 20 tons in^2, the following results are obtained (with the experimentally-determined temperatures given in parentheses):

D	:	1600	(1618) ^oK
B	:	1750	(1713) ^oK
A	:	1790	(1783) ^oK
C	:	1895	(1793) ^oK

These calculations thus correctly predict the order of sinterability and, in 3 out of 4 cases, predict the required temperature within ± 2 per cent. However, the predicted temperature for powder C is in error by 100°. The reason for this discrepancy is not understood.

It may thus be concluded that Equation 1 can be of some use in predicting the sintering behaviour of beryllia powders, and in partially explaining differences in sinterability between closely similar powders. It remains, however, a semi-empirical relationship.

The above discussion relates to prediction of sintering temperature for a target density of 2.90 g/cm^3. Figure 1 shows that, at lower densities, sintered density becomes increasingly sensitive to sintering temperature and hence any predictions would have to be exceedingly accurate (that is ± 0.5 per cent. or better) to be meaningful. It appears therefore that close control of density in these powders may only be feasible for mean densities > 2.90 g/cm^3. For example, in large-scale sintering, the accuracy of temperature control might be ± 10°C, and this would give a variation of ± 0.05 g/cm^3 in powder D with a target density of 2.80 g/cm^3 but only ± 0.005 g/cm^3 in the same powder at 2.95 g/cm^3.

4.1.3 Effect of compaction pressure (A and B only)

Equation 2 predicts a decrease in sintered density with lower green density in any one powder. Since green density decreases for both powders A and B as compacting pressure is lowered (Figure 2, lower curves), the general trend shown in the upper curves of Figure 2 is as expected. However, the superiority of powder B over A is much more pronounced than would be expected from green density differences alone and may be related to the limiting density observed with powder A (Figure 3).

A decrease in sinterability of powders A and B is observed as the compaction pressure drops below 8-10 tons/in^2 and this may be a direct result of a similar reduction in green density in this same region. To achieve a high sintered density in these powders, the compaction pressure should not be less than 7 tons/in^2.

4.1.4 Effect of milling

A milling step was introduced for powders A and D to improve the microstructure (see Section 4.2.1). No significant effects on sinterability

were expected, and none were observed.

4.2 Structure

4.2.1 Defects

Sintered compacts from each of the four powders contained undesirable microstructural features.

Powders A and B contained acicular grains or "needles" which retained their identity to quite high sintered densities (Figures 8 and 9) and these needles may affect the strength of sintered bodies.

Powder C sintered structures contained unusually pronounced triple point pores at high densities (Figure 12) and randomly dispersed coarse-grained areas (Figure 10). The latter were probably caused by impurities such as furnace refractory chips introduced during calcination from the sulphate.

Powder D structures showed variable porosity in a pattern almost certainly related to the aggregate size of the powder. The powder had been pre-compacted at 10,000 lb/in^2 and screened through a 20 mesh sieve before supply, to improve flow properties. The resultant hard granules apparently retained their identity during compaction, and the resultant lower green density at their interfaces is reflected in a lower sintered density in these areas. A simple milling operation on this powder almost completely removed between-agglomerate defects in the sintered structure and markedly improved grain size uniformity.

4.2.2 Grain size versus porosity

It has been found (Bannister 1965) for some sulphate-derived powders, that, as the surface area of the powder and green density of compacts increase, the grain size at a given sintered density decreases. The effect is quantitatively expressed by the equation :

$$P^{1.25}\, G = E = \frac{1.33\, P_o^{1.25}}{S} \quad , \qquad \ldots\ldots (2)$$

where P_o, P = green and sintered porosities (%),
E = constant,
G = grain size (μ),
S = surface area (m^2/g).

A log G versus log P plot for any one powder and green density should thus give a straight line with slope -1.25. Figure 7 is a plot of all points obtained, including all powders at 20 tons/in^2 (Figure 7a) and powders A and B at lower pressures (Figure 7b). Bands with slope -1.25 have been used to separate powders A,B, and D from powder C in Figure 7a, and to separate powder A at 20 tons/in^2 from powder A at 10 and 7 tons/in^2 and powder B at 20,10, and 7 tons/in^2 from powder B at 4 and 2 tons/in^2 in Figure 7b.

For the materials studied, the scatter in measured grain size was too large to reveal the small differences in the grain size - density relationship predicted by Equation 2, that is,

$$C_{20} > B_4 > A_7 > A_{10} > B_7 > B_{10} > A_{20} > B_{20} > D_{20} \quad ,$$

where $C_{20} : B_{20} : D_{20} = 2.4 : 1.85 : 1$.

However, this prediction is partially confirmed in the present work, but a major discrepancy is the case of D_{20}, where the grain size is much coarser than predicted.

As with Equation 1, the empirical relationship (2) appears to have a limited application in predicting the behaviour of new powders.

4.3 Strength

The strength of ceramics is closely associated with microstructure, grain size and total porosity generally being the two controlling parameters most widely and systematically studied. In practice, however, most ceramics do not have a uniform grain size or porosity distribution and 'macro' defects such as those discussed in Section 4.2 often control the strength of polycrystalline ceramics.

4.3.1 Strength - porosity relationship

Experimental evidence (Duckworth 1953; Ryshkewitch 1953) on ceramics suggests a strength-porosity relationship, for constant grain size, of the form :

$$\sigma_P = \sigma_o \exp(-BP) \quad , \qquad \ldots\ldots (3)$$

where

σ_P = modulus of rupture at porosity P ,

σ_o = modulus of rupture at zero porosity ,

B = constant.

A plot of log σ_P versus P for constant grain size is used to determine B and σ_o. Log σ_P is plotted against P for all powders in Figure 4, but as the points are not for constant grain size, B and σ_o cannot be determined. Figure 4 is however useful in comparing strength behaviour of the four powders.

Powders A and B have a higher strength than powders C and D. All strengths of powder A are greater than 30,000 lb/in^2 even at a density of 89 per cent. theoretical, but only 50 per cent. of powder B results are above 30,000 lb/in^2. Since powders A and B are nominally the same grade of beryllia, this difference in strength is unexpected and definitely undesirable.

Powder C did not form strong sintered products and 22,000 lb/in^2 was the upper strength limit attained. The strength of powder D was variable; in general it was slightly lower than that of powder B (28,000 lb/in^2 in the density range 96-98 per cent. of theoretical) but in one instance the strength was equal to that of powder A (36,000 lb/in^2 at a density of 98 per cent. of theoretical).

4.3.2 Strength-grain size relationship, powders A and B

Equation 3 has been combined by Knudsen (1959) with a strength grain size relationship :

$$\sigma = k d^{-a} \quad , \qquad \ldots\ldots (4)$$

where d = grain size

a and k = constants ,

to form the strength-grain size-density relationship :

$$\sigma_P = k d^{-a} \exp(-BP) \quad . \qquad \ldots\ldots (5)$$

The strength-grain size relationship (Equation 4) should be investigated with material having a fixed density. As this was not possible in the present work the log-log plot of Figure 5, in which powders A and B are compared, does not accurately represent Equation 4. Nevertheless the points are separated, irrespective of compacting pressure, into several

density ranges. Considering firstly powder B, it is observed that low porosity material (less than 5 per cent.) is the strongest, while high porosity materials (5 to 8 per cent.) are grouped together and are best represented by a distribution band. Typical values of 'k' in Equation 4 for low and high porosity material are 53,000 and 48,000 lb/in^2 respectively, with 'a' values of 0.36 and 0.55 respectively. The results for powder A do not fall into any marked pattern but do demonstrate the superior strength of this material over powder B, particularly at larger grain sizes.

4.3.3 Strength-compaction pressure relationship, powders A and B

The observed increase in strength with increasing green density (Figure 6) might be expected from an examination of the effect of compacting pressure on the grain size-density relationship (Figure 7). By choosing suitable conditions, compacts of low green density can be sintered to acceptable sintered densities (Figure 2), but compacting pressures greater than 4 tons/in^2 are necessary (Figure 6) to ensure high strength.

4.3.4 Effect of 'macro'-defects on strength, powders C and D

The main factor influencing the low strength of powder C and the variable strength of powder D must be the abnormal pore structure in the sintered product, in the form of 'triple' point (Figure 12) and coarse-grained/fine-grained area interface (Figure 10) porosity in powder C and between-aggregate porosity in powder D (Figure 11).

The aggregates in powder D were partially removed by a simple milling treatment described earlier, and milled powder when sintered was more uniform (Figure 14b) and noticeably stronger (Figure 4). This simple milling treatment may not be sufficient to disperse impurities in powder C which supposedly cause the large-grained areas, since this treatment was certainly not energetic enough to break acicular grains in powder A (Figure 8).

4.3.5 General remarks on the strength of powders A and B

The difference in strengths of sintered compacts from powders A and B is contrary to expectation. Since the grain size of A is larger than that of B at equivalent densities (especially for compacts of low green density), A should be weaker than B, but this is not observed.

Examination of several possible explanations of this anomaly has been inconclusive. However, since a limiting density is observed with powder A but not with powder B, it is reasonable to suspect some difference in size, shape, spacing, and position of pores between the two sintered powders. Reduced sintering rates and limiting densities are often associated with the pore isolation from grain boundaries (Burke 1957); in powder A this would be expected to commence at fairly low densities (2.84 g/cm^3) and, since the grain size is still relatively small even at a density of 2.90 g/cm^3 (Figure 7), the combined effect of a reduced number of grain boundary pores and small grain size would be beneficial to strength. Electron photomicrographs of replicas from polished and etched surfaces of sintered powders A and B are compared in Figure 15. These show the majority of pores to be at grain boundaries in both materials; however, pores are smaller and grain boundaries more irregular in powder A than in powder B.

5. SUMMARY

1. The order of sinterability of four sulphate-derived beryllia powders was correctly predicted by a semi-empirical equation which takes powder surface area and green density of the compact into account.

2. The effect of compacting pressure on the sintering behaviour of two powders (A and B) pressed at various pressures suggests that pressures higher than 7 tons/in^2 should be used to achieve high sintered density.

3. To reach the same green density, powder A required higher compacting pressures than powder B and showed a limiting sintered density at any one temperature.

4. All powders showed microstructural defects when sintered. In one powder, between-agglomerate defects, which reduced the strength, could be removed by a simple powder milling treatment and this resulted in a strength improvement. Triple point pores probably reduced the strength of another powder; the reason for the occurrence of these pores in the one powder is not known.

5. A semi-empirical equation relating sintered grain size, sintered porosity, powder surface area, and green density of the compact predicted small differences between some of the powders but these were not observed,

possibly owing to scatter of results. The equation correctly predicted the way in which grain size varied with porosity for any one powder and green density.

6. Significant differences in relative strength were noted as a function of porosity and grain size.

7. The strength versus compaction behaviour of powders A and B was consistent with the known effect of pressure on green density and on the grain size-density relationship.

8. It is postulated that the higher strength of one (A) of the two similar powders (A and B) is related to its limiting density behaviour; this may result in a reduced size and number of grain boundary pores at any particular density with consequent improvement in strength.

9. Commercial powders are of variable quality. Small but significant differences in behaviour which may arise between batches cannot be predicted accurately from any available body of knowledge, although some broad predictions can be made from a knowledge of powder surface area and compaction behaviour.

6. CONCLUSION

A simple correlation between purity and physical properties of powders, sinterability of compacts, and strength and microstructure of sintered compacts cannot be anticipated at the present stage of our knowledge of sintering of ceramics; the innumerable material and fabrication variables cannot be separated into indisputable factors of importance to the make-up of a 'perfect' grade of beryllia powder.

Commercially available powders leave much to be desired. Powders A and B are samples of the most widely used and readily available grade of beryllia on the market, but features of this powder which can be criticised are the presence of variable quantities of acicular grains, and variable compaction and sintering characteristics. Powder C is satisfactorily sinterable but the uniformity of sintered products is poor and segregated impurities in the original powder would have to be removed or dispersed before high strengths could be achieved. Powder D must be considered as a strong competitor to powders A and B. It has shown excellent properties, especially

when the powder agglomerates have been reduced by a simple milling operation. However, when large quantities and different batches of this powder are examined, the problem of lot to lot variation found with powders A and B may well apply to powder D.

7. ACKNOWLEDGEMENTS

The author is deeply indebted to Mr. L.M. Noyes who made a considerable contribution to the experiments described in this paper. The surface area measurements were made by Mr. A. Berzins, the metallographic samples were prepared by Material Physics Section, and Mr. K. Veevers was responsible for the modulus of rupture determinations.

8. REFERENCES

Bannister, M.J. (1965). - AAEC/E138.

Beaver, W.W., Theodore, J.G., and Bielawski, C.A., (1964). - J. Nucl. Mat. 14 : 326-337.

Burke, J.E. (1957). - J. Amer. Ceram. Soc. 40 : 80-85.

Duckworth, W.J. (1953). - J. Amer. Ceram. Soc. 36 : 68.

Knudsen, F.P. (1959), - J. Amer. Ceram. Soc. 42 : 376.

Livey, D.T., and Hey, A.W. (1964). - J. Nucl. Mat. 14 : 285-293.

Reeve, K.D., and Ramm, E.J. (1961). - AAEC/E80.

Reeve, K.D., and Bridgford, K.C. (1964). - AAEC/TM255.

Ryshkewitch, E. (1953). - J. Amer. Ceram. Soc. 36 : 65.

Veevers, K., and Rotsey, W.B. (1965). - AAEC/TM290.

APPENDIX 1

DETERMINATION OF POUR DENSITY AND TAP DENSITY OF BeO POWDERS

Equipment — Balance, Graduate (100ml), Funnel (4 in. dia.)
Ring Stand (3 in. dia.)

Procedure

Adjust the ring on the stand so that the powder funnel resting on the stand will have exactly 3 inches between the bottom of the funnel and the top of the graduate. The funnel is filled with oxide while keeping a finger over the bottom of the funnel. The oxide is then allowed to flow freely from the funnel into a previously weighed graduate of the known total volume until the graduate is full to overflowing. The oxide is then sliced off level with a spatula and the graduate is wiped clean of oxide from the outside surfaces. The graduate is then weighed and the pour density is calculated.

The graduate is tapped by hand until there is no visual evidence of further reduction of volume of the oxide. The graduate is then reweighed to confirm previous weight and also to confirm no loss of oxide. The volume of the oxide is read directly from the graduate and the tap density is calculated.

Calculations

$$\text{Pour density} = \frac{\text{Weight of oxide}}{\text{Volume of graduate}}$$

$$\text{Tap density} = \frac{\text{Weight of oxide}}{\text{Volume of oxide}}$$

TABLE 1

SOURCES AND ANALYSES OF BERYLLIA POWDERS

(all analyses in p.p.m.)

Powder	A		B		C	D	
Source	Brush Beryllium Co. U.S.A.		Brush Beryllium Co. U.S.A.		Pechiney Cie France	NGK Insulators, Japan	
Grade	UOX Lot 200-W-266-P		UOX Lot 200-W-269-P		PY 60	CF Lot 907-21	
	(a)	(b)	(a)	(b)	(a) (b)	(a)	(b)
Al	50		55		80	10	
Fe	25		20		25	<10	
Si	45		45		25	85	
Mg	50		50		10	15	
Mn	3		5			< 5	
Cr	9		4		<20	< 5	
Ni	7		< 3		<20	< 4	
Zn		<35		<35	<35		
Na	30		10		<35	36	
Ca	<30		<30		<20	90	
C		310		600	340		
F		< 5			< 5		
S		740		938	1470	830	

Note: (a) = supplier's analysis
(b) = A.A.E.C. analysis

TABLE 2

PHYSICAL PROPERTIES

Powder	Surface Area (m^2/g)	Pour Density (g/cm^3)	Tap Density (g/cm^3)	Green Density (g/cm^3)	Shape, Size, and Agglomeration of Powders
A	9.5	0.34	0.45	1.78	loose aggregates of sub-micron crystallites plus acicular grains up to 200 microns long x 40 microns wide
B	9.7	0.30	0.53	1.82	ditto
C	8.1	0.19	0.31	1.72	loose aggregates of sub-micron crystallites
D	20.0	0.74	0.94	1.70	ditto plus 'hard' 5-500 micron aggregates

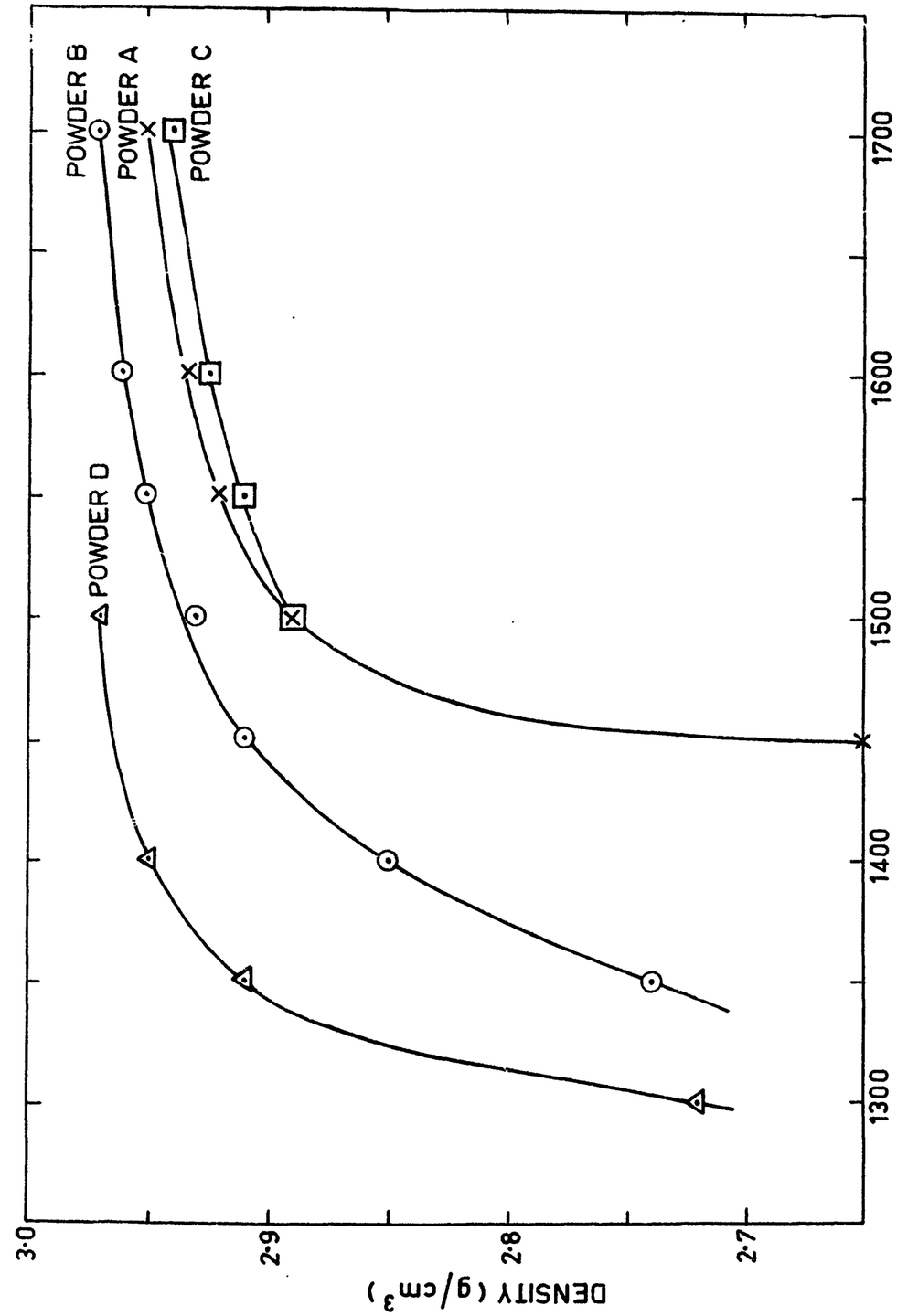

FIGURE 1. DENSITY AFTER SINTERING AT TEMPERATURE FOR ONE HOUR

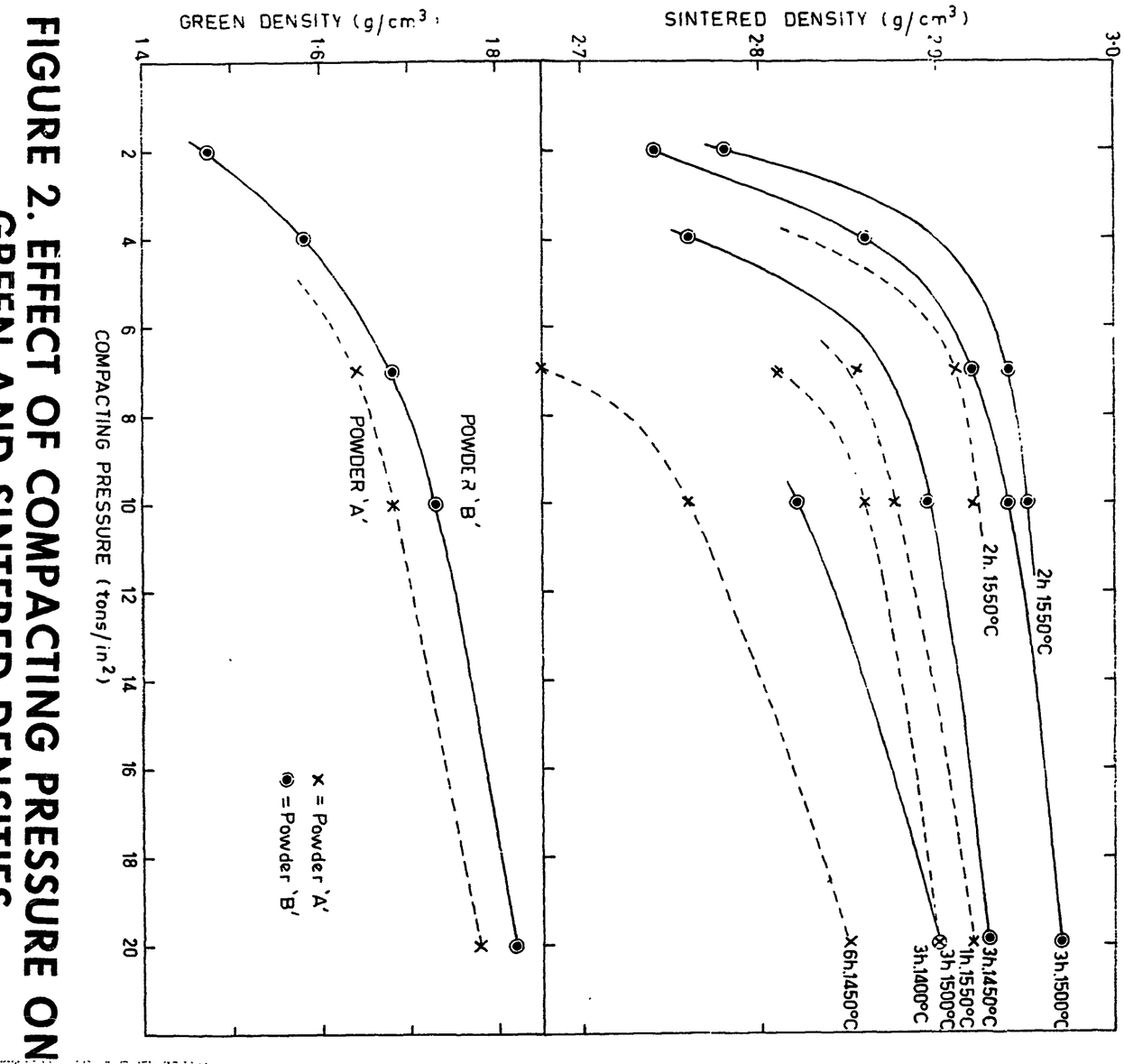

FIGURE 2. EFFECT OF COMPACTING PRESSURE ON GREEN AND SINTERED DENSITIES OF POWDERS A AND B

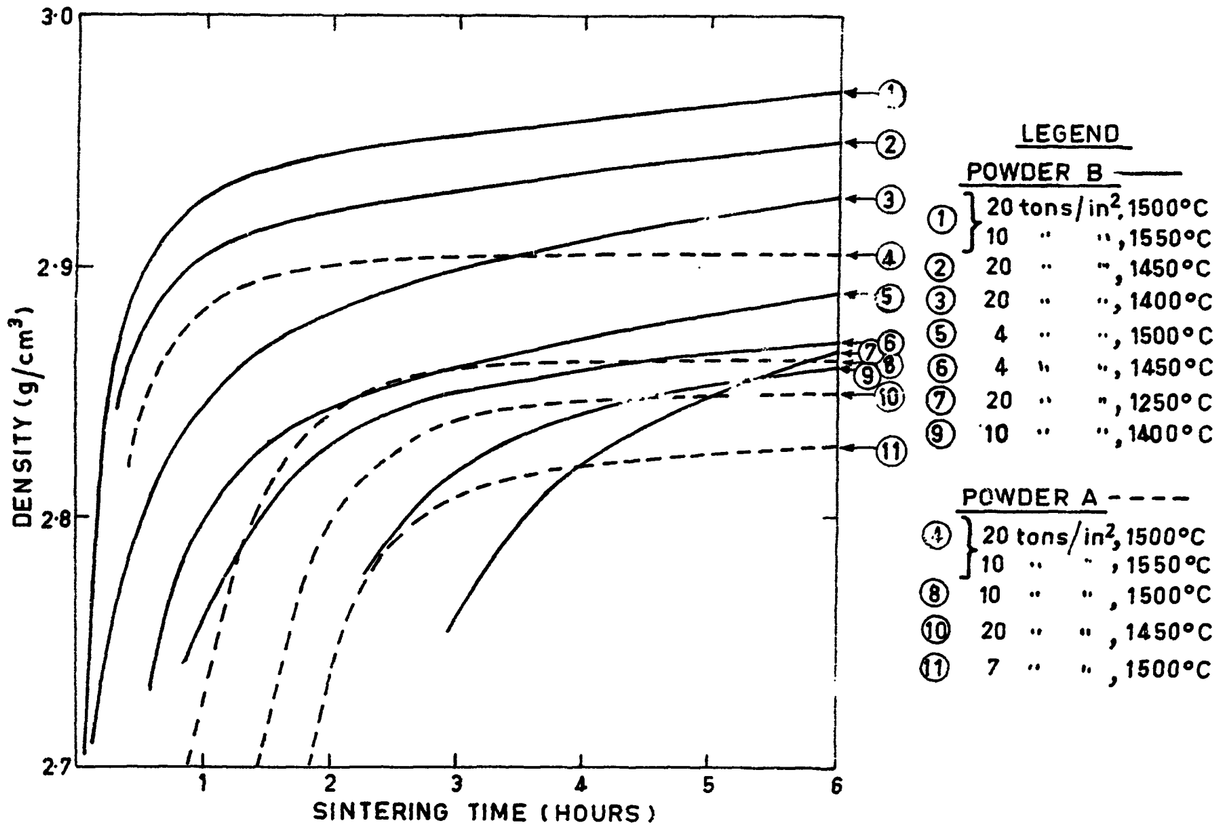

FIGURE 3. A COMPARISON OF THE SINTERABILITY OF POWDERS A AND B

P969

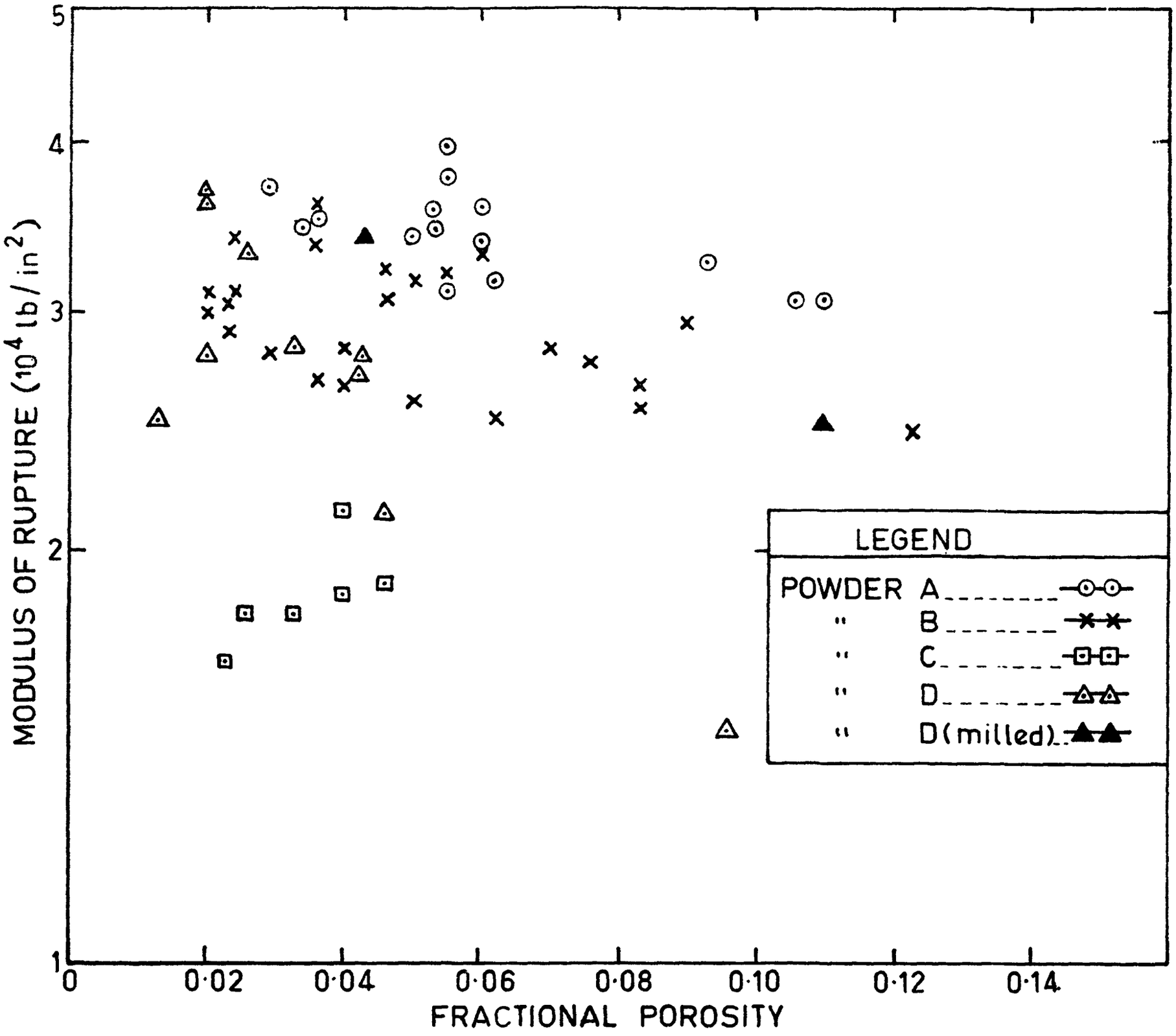

FIGURE 4. MODULUS OF RUPTURE vs POROSITY

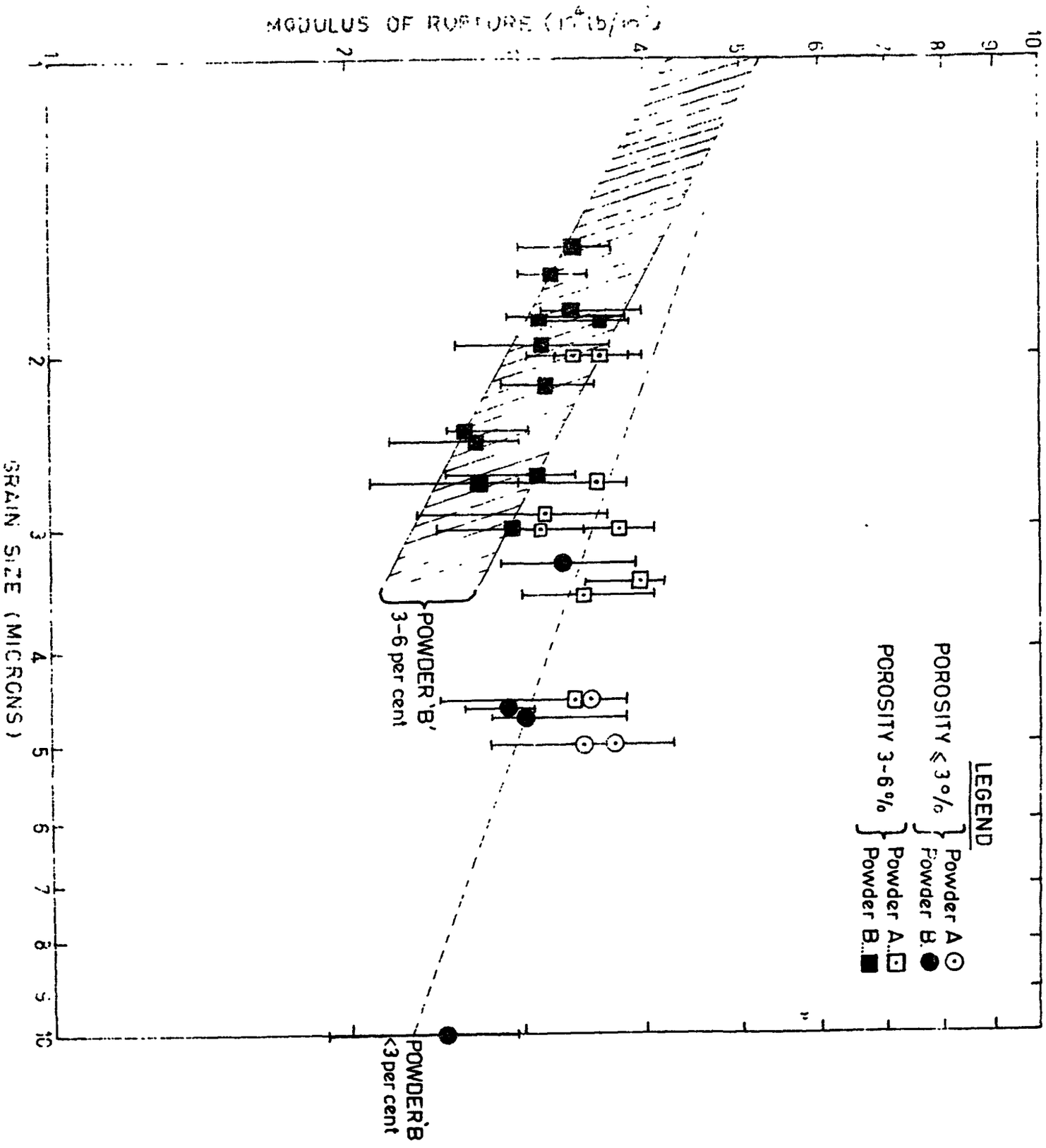

FIGURE 5. MODULUS OF RUPTURE vs GRAIN SIZE

P96?

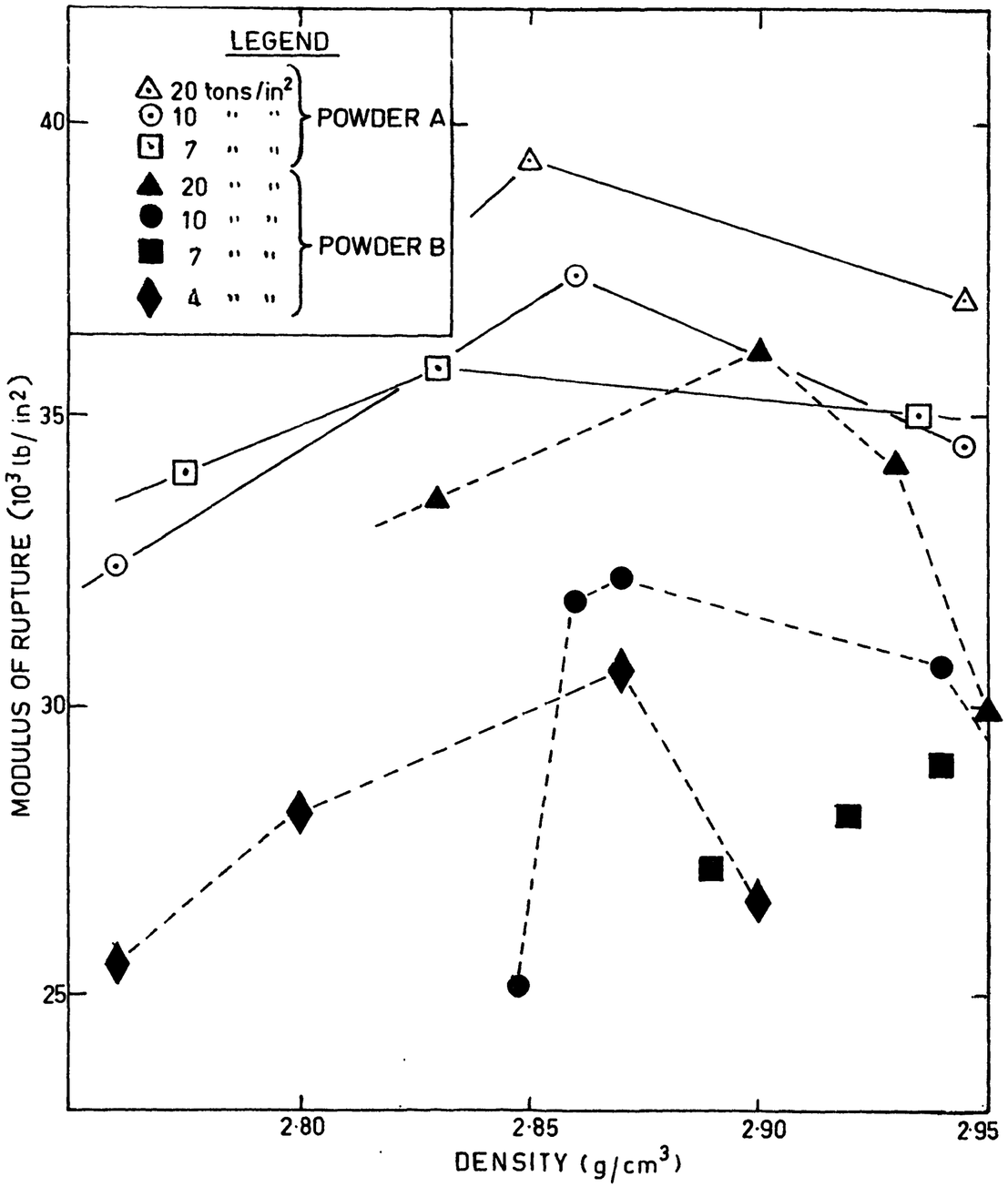

FIGURE 6. EFFECT OF COMPACTING PRESSURE ON MODULUS OF RUPTURE OF POWDERS A AND B

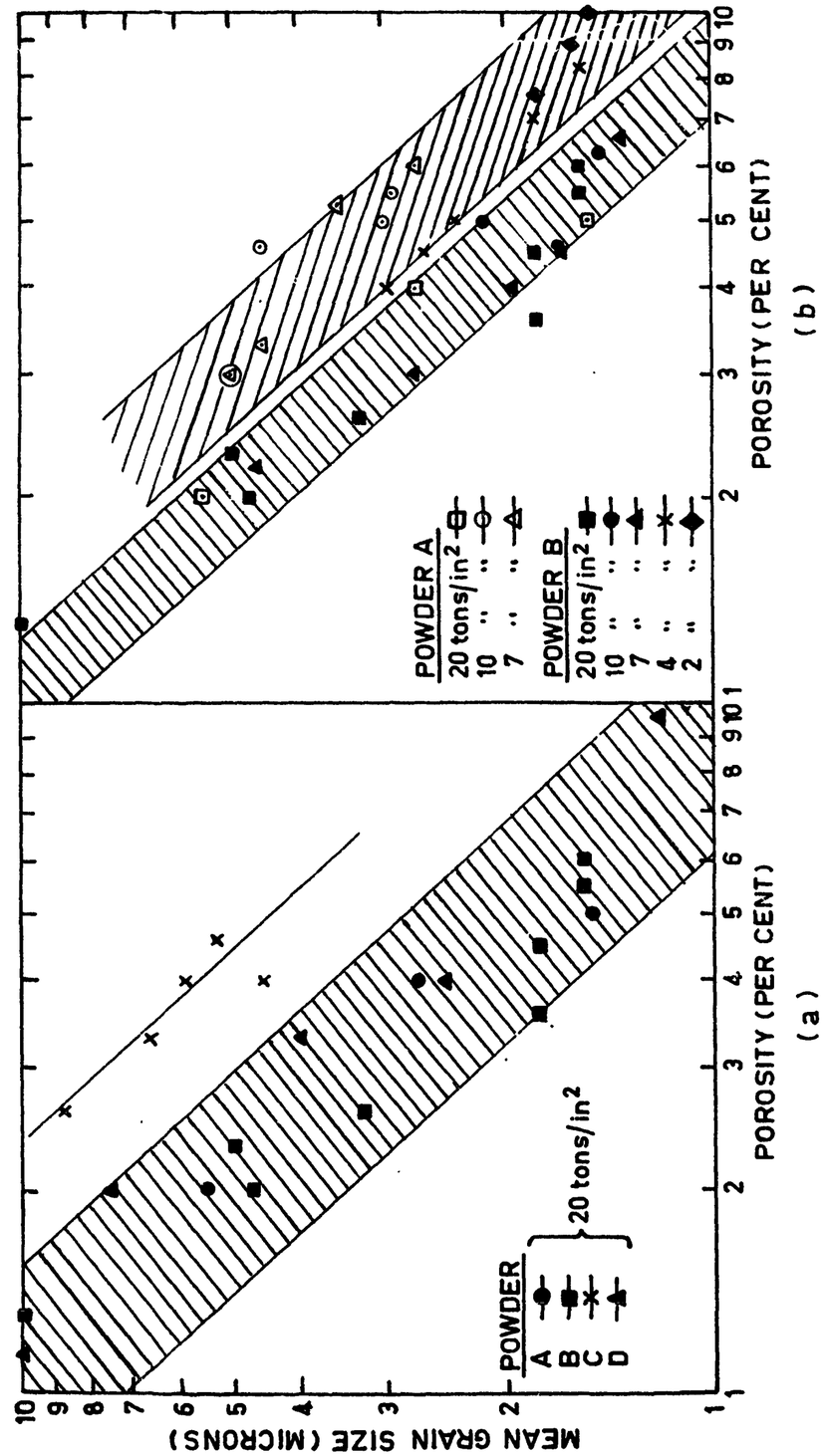

FIGURE 7. GRAIN SIZE vs POROSITY

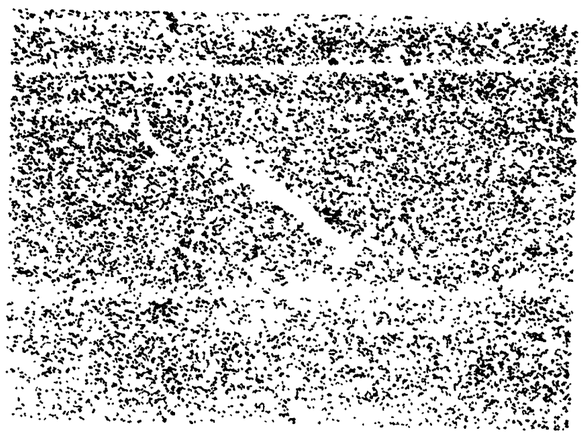

×250

FIGURE 8. POWDER A SINTERED FOR 3h AT 1450° C, DENSITY 2.85g/cm^3

×25

FIGURE 9. POWDER B SINTERED FOR 6h AT 1350° C, DENSITY 2.87g/cm^3

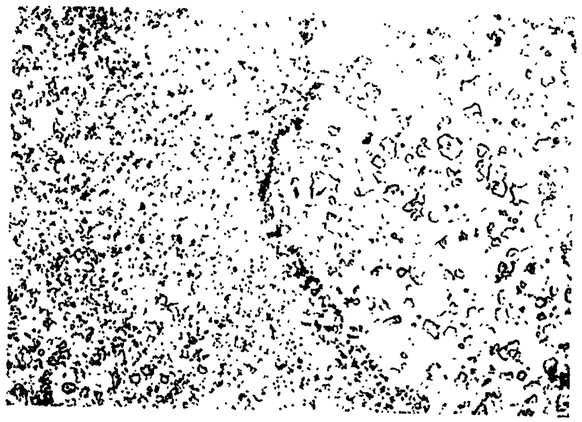

×250

FIGURE 10. POWDER C SINTERED FOR 3h AT 1450° C, DENSITY 2.87g/cm^3

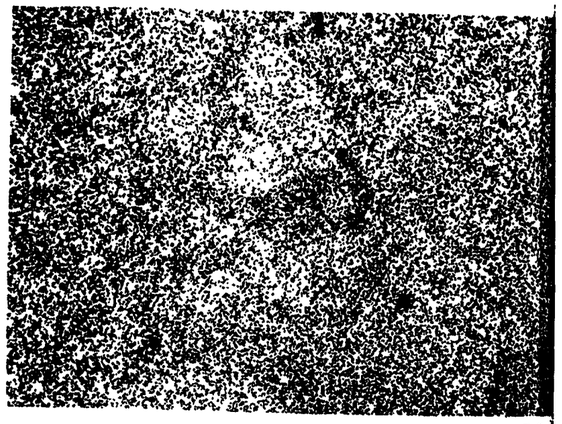

×250

FIGURE 11. POWDER D SINTERED FO 2h AT 1315° C, DENSITY 2.87g/cm^3

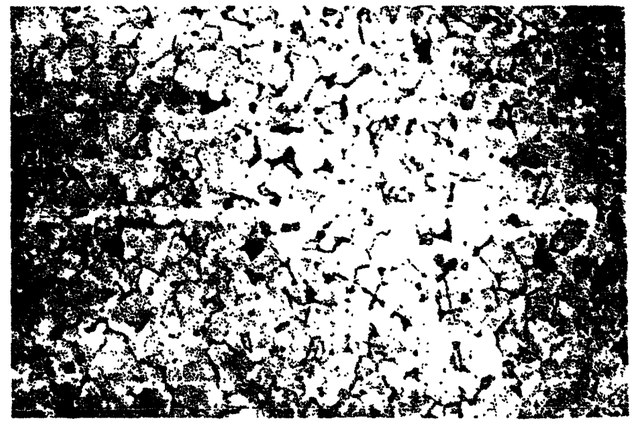

×500

FIGURE 12. POWDER C DENSITY 2.93g/cm^3
GRAIN SIZE 9 microns
MODULUS OF RUPTURE 17,875lb/in^2

×500

FIGURE 13. POWDER B DENSITY 2.95g/cm^3
GRAIN SIZE 7 microns
MODULUS OF RUPTURE 30,090lb/in^2

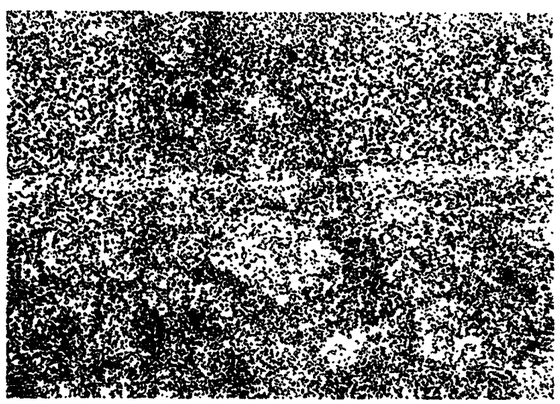

×250

×75

a) AS-RECEIVED

×250

×75

b) MILLED

FIGURE 14. POWDER D PRESSED AT 20 tons/in^2, SINTERED TO A DENSITY OF 2.87g/cm^3

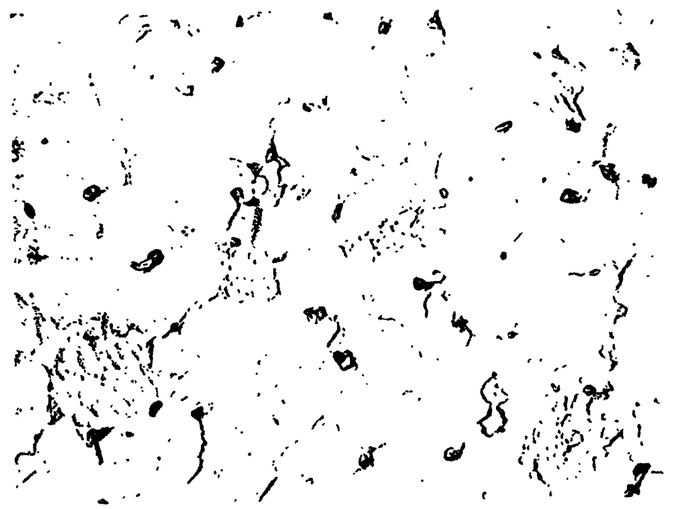

×4000

(POWDER A, DENSITY 2.92g/cm^3)

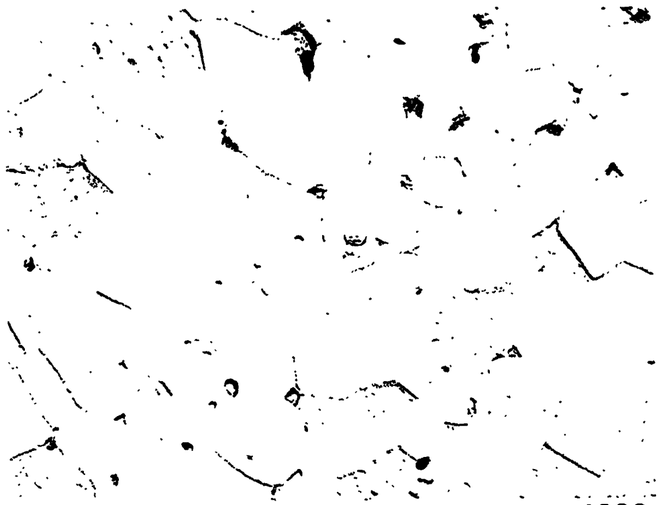

×4000

(POWDER B, DENSITY 2.95g/cm^3)

FIGURE 15. ELECTRON PHOTOMICROGRAPHS OF POWDERS A AND B PRESSED AT 20 tons/in^2 AND SINTERED